



**gp130 in late osteoblasts and osteocytes is required for PTH-induced osteoblast differentiation**

Journal:	<i>Journal of Endocrinology</i>
Manuscript ID:	JOE-14-0424.R1
Manuscript Type:	Research Paper
Date Submitted by the Author:	n/a
Complete List of Authors:	Standal, Therese; St. Vincent's Institute, Bone Cell Biology & Disease Johnson, Rachelle; St. Vincent's Institute, Bone Cell Biology & Disease McGregor, Narelle; St. Vincent's Institute, Bone Cell Biology & Disease Poulton, Ingrid; St. Vincent's Institute, Bone Cell Biology & Disease Ho, Patricia; St. Vincent's Institute, Bone Cell Biology & Disease Martin, T John; St. Vincent's Institute of Medical Research, Bone Cell Biology and Disease Unit Sims, Natalie; St. Vincent's Institute of Medical Research, Bone Cell Biology & Disease
Keywords:	Parathyroid hormone, Osteoblast, Interleukins, Osteoclast

SCHOLARONE™  
Manuscripts

Only

1 **gp130 in late osteoblasts and osteocytes is required for PTH-induced**  
2 **osteoblast differentiation**

3 *Therese Standal<sup>1,3</sup>, Rachelle W Johnson<sup>1</sup>, Narelle E McGregor<sup>1</sup>, Ingrid J Poulton<sup>1</sup>,*

4 *Patricia W M Ho<sup>1</sup>, T. John Martin<sup>1,2</sup> and Natalie A Sims<sup>1,2</sup>*

5 <sup>1</sup>St.Vincent's Institute of Medical Research, Fitzroy, Victoria, Australia

6 <sup>2</sup>The University of Melbourne, Department of Medicine at St. Vincent's Hospital

7 Melbourne, Fitzroy, Victoria, Australia

8 <sup>3</sup>The KG Jebsen Center for Myeloma Research and Centre of Molecular

9 Inflammation Research, Department of Cancer Research and Molecular Medicine,

10 Norwegian University of Science and Technology, Trondheim, Norway

11 Short title: osteocytic gp130 and PTH anabolic response

12 Corresponding author:

13 Natalie A Sims

14 9 Princes St

15 Fitzroy, Victoria 3122

16 Australia

17 Email: [nsims@svi.edu.au](mailto:nsims@svi.edu.au)

18 Phone: +613-9288-2555

19 Fax: +613-9416-2676

20 Abstract: 223 words

21 Manuscript: 3718

22 Key words: glycoprotein-130 (gp130), osteoblast, osteocyte, osteoclast, PTH,

23 PTH1R, trabecular, cortical, bone formation

## 24 **Abstract**

25 Parathyroid hormone (PTH) treatment stimulates osteoblast differentiation and  
26 bone formation, and is the only currently approved anabolic therapy for  
27 osteoporosis. In cells of the osteoblast lineage, PTH also stimulates expression of  
28 members of the IL-6 cytokine superfamily. Although the similarity of gene  
29 targets regulated by these cytokines and PTH suggest cooperative action, the  
30 dependence of PTH anabolic action on IL-6 cytokine signaling is unknown.  
31 To determine whether cytokine signaling in the osteocyte through glycoprotein  
32 130 (gp130), the common IL-6 superfamily receptor subunit, is required for PTH  
33 anabolic action, male mice with conditional gp130 deletion in osteocytes  
34 (*Dmp1Cre.gp130<sup>ff</sup>*) and littermate controls (*Dmp1Cre.gp130<sup>w/w</sup>*) were treated  
35 with hPTH(1-34) (30µg/kg 5x/week for 5 weeks). PTH dramatically increased  
36 bone formation in *Dmp1Cre.gp130<sup>w/w</sup>* mice, as indicated by elevated osteoblast  
37 number, osteoid surface, mineralizing surface, and increased serum N-terminal  
38 propeptide of type I collagen (P1NP). However, in mice with DMP1Cre-directed  
39 deletion of gp130, PTH treatment changed none of these parameters.  
40 Impaired PTH anabolic action was associated with a 50 percent reduction of  
41 *Pth1r* mRNA levels in *Dmp1Cre.gp130<sup>ff</sup>* femora compared to *Dmp1Cre.gp130<sup>w/w</sup>*.  
42 Furthermore, lentiviral cre infection of *gp130<sup>ff</sup>* primary osteoblasts also lowered  
43 *Pth1r* mRNA levels to 16% of that observed in infected C57/BL6 cells.  
44 In conclusion, osteocytic gp130 is required to maintain PTH1R expression in the  
45 osteoblast lineage, and for the stimulation of osteoblast differentiation that  
46 occurs in response to PTH.

## 47 **Introduction**

48 Intermittent administration of parathyroid hormone (PTH) to animal models and  
49 humans (Teriparatide (Forteo)) increases bone mass (Lindsay, et al. 2007; Neer,  
50 et al. 2001; Reeve, et al. 1980), and is the only approved treatment for  
51 osteoporosis capable of inducing bone formation (reviewed in (Hodsman, et al.  
52 2005; Khosla, et al. 2008)). However, the mechanisms by which intermittent PTH  
53 increases bone mass remain unclear, and identifying downstream targets of this  
54 pathway may aid in the design of improved anabolic therapies.

55

56 The effects of PTH on bone mass are likely to be mediated by cells of the  
57 osteoblast lineage. This lineage includes committed pre-osteoblasts, matrix-  
58 producing osteoblasts, bone lining cells, and matrix-embedded osteocytes. PTH  
59 acts directly at each stage of differentiation, as follows. PTH promotes pre-  
60 osteoblast differentiation (Dobnig and Turner 1995), inhibits osteoblast  
61 apoptosis (Jilka, et al. 1999), and reactivates quiescent lining cells to become  
62 active osteoblasts (Kim, et al. 2012). PTH also acts directly on osteocytes to  
63 reduce their expression of the Wnt antagonist sclerostin, an inhibitor of bone  
64 formation (Bellido, et al. 2005; Keller and Kneissel 2005).

65

66 PTH **also** stimulates expression of receptor activator of NF-kappa-B ligand  
67 (RANKL) by early osteoblast lineage cells, thereby promoting osteoclast  
68 differentiation (Udagawa, et al. 1999). However, the stages of osteoblast  
69 differentiation most important for the actions of PTH remain controversial, since

70 expression of RANKL by matrix-embedded osteocytes is also stimulated by PTH  
71 (Xiong, et al. 2011).

72

73 PTH also acts on the osteoblast lineage to rapidly promote expression of IL-6  
74 family cytokines and receptors. These include interleukin-6 (IL-6) (Greenfield, et  
75 al. 1996), interleukin-11 (IL-11), oncostatin M (OSM) receptor (OSMR), leukemia  
76 inhibitory factor (LIF) and cytokine receptor-like factor 1 (CRLF1)(Walker, et al.  
77 2012). These cytokines all depend on the promiscuous co-receptor gp130 for  
78 signaling (reviewed in (Sims and Walsh 2010)), and gp130 expression by the  
79 osteoblast lineage is also stimulated by PTH (Romas, et al. 1996).

80

81 Many of the actions and gene targets of IL-6 family cytokines are common to  
82 those of PTH. As is the case with PTH, the cytokines IL-6, IL-11, OSM, LIF and  
83 cardiotrophin (CT-1) promote osteoblast differentiation *in vitro* (Walker, et al.  
84 2008; Walker, et al. 2010) and OSM, LIF and CT-1 stimulate bone formation *in*  
85 *vivo* (Cornish, et al. 1993; Walker et al. 2008; Walker et al. 2010). Family  
86 members IL-11, LIF, OSM, CT-1 and CNTF also inhibit osteocytic sclerostin  
87 expression (Johnson, et al. 2014b; Walker et al. 2010). In addition, IL-6, IL-11,  
88 OSM, LIF and CT-1 stimulate osteoblast lineage expression of RANKL (O'Brien, et  
89 al. 1999; Palmqvist, et al. 2002; Walker et al. 2008) and promote  
90 osteoclastogenesis when precursors are co-cultured with osteoblasts *in vitro*  
91 (Richards, et al. 2000; Tamura, et al. 1993). These similar effects, and the  
92 upregulation of IL-6 family cytokines in osteoblasts by PTH suggest that this  
93 cytokine family may play a role in the actions of PTH on the osteoblast lineage.

94

95 Hence, in this study we examined the requirement of gp130 signaling in

96 osteocytes for the anabolic action of PTH, using mice with DMP1Cre-directed

97 deletion of gp130 in osteocytes (*Dmp1Cre.gp130<sup>fl/fl</sup>*) (Johnson, et al. 2014a) and

98 mature osteoblasts (Torreggiani, et al. 2013; Xiong et al. 2011). We found that

99 gp130 in these cells is required for PTH to increase osteoblast number and bone

100 forming surfaces, and to maintain PTH1R expression in the osteoblast lineage.

101

For Review Only

## 102 **Materials and methods**

### 103 *Mice*

104 All animal procedures were conducted with approval of the St. Vincent's Health  
105 Melbourne Animal Ethics Committee. DMP1Cre mice were obtained from Lynda  
106 Bonewald (University of Kansas, Kansas City, USA) (Lu, et al. 2007). Floxed  
107 gp130 mice backcrossed onto C57/BL6 were obtained from Rodger McEver  
108 (Oklahoma Medical Research Foundation) (Betz, et al. 1998). Mice hemizygous  
109 for the Cre transgene were crossed with the gp130 flox mouse in which the  
110 transmembrane domain (exon 15) was flanked by loxP sites, resulting in ablation  
111 of intracellular gp130 signalling, as previously reported (Betz et al. 1998) and  
112 confirmed **at the mRNA level** in bone (Johnson et al. 2014a). For all experiments,  
113 DMP1.Cre+ cousins were used as controls.

114

115 Six week old male DMP1Cre+gp130 wildtype (*Dmp1Cre.gp130<sup>w/w</sup>*) or  
116 DMP1Cre+gp130 floxed (*Dmp1Cre.gp130<sup>f/f</sup>*) mice were injected i.p. with 30µg/kg  
117 human parathyroid hormone 1-34 (hPTH 1-34) or vehicle 5 days a week for 5  
118 weeks (n=9/10 per group). **This dose and duration of PTH treatment was chosen**  
119 **because it provides a robust increase in lamellar bone formation rate and**  
120 **osteoblast surface in male mice without increasing osteoclastogenesis (Takyar,**  
121 **et al. 2013; Tonna, et al. 2014; Walker et al. 2012).** Mice were also injected with  
122 calcein (20mg/kg) 7 and 2 days prior to tissue collection. Bones were collected  
123 one hour after the last PTH injection. The mice were fasted for 12 hours prior to  
124 anaesthesia with ketamine/xylazine and a final blood sample was collected by

125 cardiac puncture. Blood samples were centrifuged for 10 minutes at 4,000 rpm  
126 and serum was removed to a fresh tube and stored at -80°C until analysis for  
127 cross-linked C-terminal telopeptide of type I collagen (CTX-1), N-terminal  
128 propeptide of type I collagen (P1NP) (Immunodiagnostic Systems Limited,  
129 Boldon, Tyne & Wear, UK) and PTH (Immunotopics, San Clemente, CA) as per  
130 manufacturer's instructions. One femur was flushed of marrow and the bone  
131 shaft was collected for RNA analyses as previously described (Walker et al.  
132 2012). Briefly, bones were homogenized with a LS-10-35 Polytron homogenizer  
133 in Trizol for 4 x 5 second bursts and stored at -80C. RNA from each bone was  
134 purified using the RNeasy lipid tissue minikit (Qiagen), according to  
135 manufacturer's instructions.

136

137 The other femur was analysed by micro-computed tomography as previously  
138 described (Johnson et al. 2014a) using the SkyScan 1076 system (Bruker-  
139 microCT, Kontich, Belgium). Images were acquired using the following settings:  
140 9µm voxel resolution, 0.5mm aluminium filter, 48kV voltage and 100µA current,  
141 exposure time, rotation 0.5°, frame averaging =1. Images were reconstructed  
142 and analysed using SkyScan software programs NRecon (version 1.6.3.3),  
143 DataViewer (version 1.4.4) and CT Analyser (version 1.12.0.0). Femoral  
144 trabecular analysis region of interest (ROI) was determined by identifying the  
145 distal end of the femur and calculating 15% of the total femur length towards the  
146 femora mid-shaft, where we then analysed an ROI of 12.6% of the total femur  
147 length. Analysis of bone structure was completed using adaptive thresholding  
148 (mean of min and max values) in CT Analyser. Thresholds for analysis were



149 determined based on multilevel Otsu thresholding of the entire data set, and  
150 were set at 45-255 for trabecular bone. Cortical analyses were performed 35%  
151 above the distal end of the femur toward the femora mid-shaft, also with a 12.6%  
152 ROI with the threshold values set at 100-255.

153

154 Tibiae were collected for histomorphometric analyses as previously described  
155 (Sims, et al. 2006). Briefly, trabecular histomorphometry was carried out on  
156 undecalcified sections in the secondary spongiosa of the proximal tibia, in a  
157 region 370µm below the proximal edge of the hypertrophic zone of the growth  
158 plate, extending 1.11 mm in the proximal direction. Periosteal  
159 histomorphometry was carried out on the antero-fibular side of the tibia,  
160 commencing 1.11mm below the chondro-osseus junction of the growth plate,  
161 and extending 1.11 mm in the proximal direction. Nomenclature is as previously  
162 described (Parfitt, et al. 1987).

163

164 *Lenti-cre viral infection*

165 Calvarial osteoblasts were collected from C57/BL6 wildtype and *gp130<sup>ff</sup>*  
166 neonates by digesting calvaria in 1:2 collagenase II/dispase solution at 37°C on a  
167 shaker (1 x 5 minutes, 4 x 10 minute digestions). The cells were resuspended in  
168 culture media, and allowed to adhere overnight before being frozen and stored  
169 in liquid nitrogen. When required, isolated cells were thawed and expanded in  
170 culture and infected with a GFP-tagged lenti-Cre virus synthesised as previously  
171 described (Tonna et al. 2014) for 24 hours with polybrene in maintenance  
172 media. Following infection, media was changed and cells were evaluated for GFP

173 expression by microscopy; >30-60% transfection efficiency was observed (n=3  
174 independent experiments). Cells were expanded in culture for 2-3 weeks in  
175 maintenance media and GFP positive cells (fluorescence driven by Cre transgene  
176 expression) were sorted on a FACS Aria (BD Biosciences, San Jose, California) for  
177 GFP. Sorted cells were harvested for RNA in Trizol (Life Technologies, Carlsbad,  
178 California) and separated and precipitated using chloroform and isopropanol.  
179 Extracted RNA was DNase treated using Ambion TURBO DNA-free kit (Life  
180 Technologies) and quantified on a NanoDrop ND1000 spectrophotometer  
181 (Thermo Scientific, Wilmington, DE).

182

### 183 *Semi-quantitative real-time PCR (qPCR)*

184 cDNA synthesis from 50-100 ng DNase-treated RNA **from each femur or cell**  
185 **culture preparation** was performed using AffinityScript (Agilent Technologies,  
186 Santa Clara, California, USA) per the manufacturer's instructions. Stock cDNA  
187 was diluted to a concentration of 5 ng/ $\mu$ l and semi-quantitative real-time PCR  
188 was performed on 12.5 ng cDNA in a reaction volume of 10  $\mu$ l using in-house  
189 master mix of 10X AmpliTaq Gold with SYBR Green nucleic acid gel stain (Life  
190 Technologies). *Dkk1* primers were designed using NCBI Primer Blast: Forward-  
191 GAGGGGAAATTGAGGAAAGC; Reverse-ACGGAGCCTTCTTGTCCCTT. Other  
192 primers were as previously described for *Pth1r*, *Hprt1*, *Sost*, *Tnfsf11*, *Il6* (Allan, et  
193 al. 2008), *B2m* (McGregor, et al. 2010), and *Hmbs* (Johnson et al. 2014a).

194

195 Samples were dispensed onto optically clear 96-well plates (Thermo Scientific)  
196 and run on a Stratagene Mx3000P (Agilent Technologies). Cycling conditions

197 were 95°C for 10 min, (95°C for 30 sec, 58°C for 1min, 72°C for 30 sec) X 40 cycles,  
198 followed by dissociation step (95°C for 1min, 55°C for 30 sec, 95°C for 30 sec).  
199 Post-run samples were analysed using Stratagene software MxPro and reported  
200 using linear  $\Delta$ CT values normalized to the geometric mean of the two  
201 housekeeping genes (HKG) hypoxanthine phosphoribosyltransferase 1 (*Hprt1*)  
202 and hydroxymethylbilane synthase (*Hmbs*) or to  $\beta$ -2 microglobulin (*B2m*) as  
203 indicated.

204

#### 205 *Statistics*

206 All graphs are presented as the mean/genotype + standard error of the mean. N  
207 = 5-10 animals/group as indicated on the graph or in the figure legend. For *in*  
208 *vitro* experiments, data shown is the average of 3 independent biological  
209 replicates. Statistical significance was considered when  $p < 0.05$ . In all figures  
210 \*= $p \leq 0.05$ , \*\*= $p \leq 0.01$ , \*\*\*= $p \leq 0.001$ . Differences between groups were analysed  
211 by 2-way ANOVA and post hoc Šidak multiple comparison test. Skewed variables  
212 (mRNA data in Figure 4) were transformed using the natural logarithm before  
213 statistical analyses. For the lenti-viral Cre infected primary calvarial osteoblasts,  
214 Student's t-test was used to assess significance. Statistical analyses were  
215 performed using GraphPad Prism version 6.0c for Mac OS X (GraphPad Software,  
216 La Jolla, California, USA).

217

## 218 **Results**

219 *Dmp1Cre.gp130<sup>ff</sup>* mice show no increase in trabecular osteoblast number in

220 response to PTH

221

222 PTH treatment at 30µg/kg/day significantly increased osteoblast number / bone

223 perimeter (NOb/BPm) on trabecular bone in *Dmp1Cre.gp130<sup>w/w</sup>* mice by 76%

224 (Figure 1A). Osteoblast surface / bone surface (ObS/BS) (Figure 1B) and osteoid

225 surface / bone surface (OS/BS)(Figure 1C) were also elevated by PTH treatment

226 to similar extents. We detected no significant changes in osteoid thickness in

227 *Dmp1Cre.gp130<sup>w/w</sup>* mice after PTH treatment (Figure 1D).

228

229 In contrast to *Dmp1Cre.gp130<sup>w/w</sup>* mice, PTH treatment did not increase

230 osteoblast or osteoid-derived parameters in age- and sex-matched

231 *Dmp1Cre.gp130<sup>ff</sup>* mice (Figure 1A-D). Two-way ANOVA revealed that the effects

232 of PTH treatment on both NOb/BPm and ObS/BS were significantly reduced in

233 the *Dmp1Cre.gp130<sup>ff</sup>* mice compared to *Dmp1Cre.gp130<sup>w/w</sup>* controls (interaction

234  $p=0.039$ , and  $0.043$ , respectively). This indicates that the effect of PTH on

235 osteoblast differentiation is dependent on gp130 expression in osteocytes.

236

237 In line with the effects on osteoblast numbers, bone forming surfaces, indicated

238 by incorporation of calcein labels, including both double labeled surface (Figure

239 1E) and single labeled surface ( $p\leq 0.05$ , not shown) were significantly greater in

240 PTH treated *Dmp1Cre.gp130<sup>w/w</sup>* mice compared to controls. Again, this was not

241 observed in *Dmp1Cre.gp130<sup>ff</sup>* mice. Mineral apposition rate (MAR) was  
242 significantly greater in both *Dmp1Cre.gp130<sup>ff</sup>* and *Dmp1Cre.gp130<sup>w/w</sup>* mice  
243 treated with PTH compared to their vehicle-treated controls (Figure 1F),  
244 indicating that an increase in mineralization rate in response to PTH is retained  
245 on those surfaces on which bone formation occurs in *Dmp1Cre.gp130<sup>ff</sup>* mice.  
246  
247 PTH treated *Dmp1Cre.gp130<sup>w/w</sup>* mice had significantly higher serum P1NP levels  
248 than *Dmp1Cre.gp130<sup>w/w</sup>* untreated controls. In contrast, in *Dmp1Cre.gp130<sup>ff</sup>* mice  
249 there was no significant effect of PTH on P1NP levels compared to vehicle-  
250 treated *Dmp1Cre.gp130<sup>ff</sup>* mice (Figure 1G); interaction p-value=0.009 by two-  
251 way ANOVA. These results are consistent with the histomorphometry data and  
252 confirm that at a systemic level, the effect of PTH on bone formation is blunted in  
253 *Dmp1Cre.gp130<sup>ff</sup>* mice.

254  
255 In both *Dmp1Cre.gp130<sup>ff</sup>* and *Dmp1Cre.gp130<sup>w/w</sup>* mice, intermittent human PTH  
256 treatment led to reduced production of endogenous circulating murine PTH  
257 levels (Figure 1H), demonstrating that negative feedback at the parathyroid  
258 induced by exogenous PTH administration was maintained in both groups of  
259 mice.

260  
261 **Although this dose of PTH significantly increased all markers of bone formation**  
262 **in *Dmp1Cre.gp130<sup>w/w</sup>* mice, we did not detect a significant increase in trabecular**  
263 **bone mass by micro-computed tomography with this short time course of low**  
264 **dose treatment (Table 1).**

265

266 *No effect of intermittent PTH treatment on bone resorption*

267 This protocol of intermittent PTH treatment did not significantly change

268 osteoclast number / bone perimeter (NOc/BPm) (Figure 2A), osteoclast surface

269 / bone surface (OcS/BS) (Figure 2B) or serum levels of cross-linked C-terminal

270 telopeptide of type I collagen (CTX1) (Figure 2C) in either *Dmp1Cre.gp130<sup>ff</sup>* or271 *Dmp1Cre.gp130<sup>w/w</sup>* mice. This confirms our previous observations using similar

272 protocols over 4 weeks of treatment (Takyar et al. 2013; Tonna et al. 2014;

273 Walker et al. 2012).

274

275 *Effects of PTH on cortical bone*

276 Although periosteal double labeled surface (dLS/BS) was not altered by PTH

277 treatment in either genotype (Figure 3A), periosteal mineral apposition rate

278 (Figure 3B) and periosteal perimeter (Figure 3C) were all significantly greater in

279 PTH-treated *Dmp1Cre.gp130<sup>w/w</sup>* mice compared with untreated mice. None of

280 these parameters were significantly increased by PTH treatment in

281 *Dmp1Cre.gp130<sup>ff</sup>* mice compared to genotype-matched vehicle controls (Figure

282 3B), indicating that periosteal growth in response to PTH may also be impaired

283 in the absence of osteocytic gp130.

284

285 *Normal response of osteoclastic genes, but lack of inhibition of Wnt signaling*286 *inhibitors by PTH treatment in DMP1Cre.gp130<sup>ff</sup> mice*287 RANKL (gene name *Tnfsf11*) and IL-6 (*Il6*) are both potent stimuli of osteoclast

288 formation, and PTH increases their expression in cells of the osteoblast lineage

289 (Greenfield, et al. 1995; Udagawa et al. 1999). Indeed, in marrow-flushed femoral  
290 samples collected 1 hour after the last of these 5 weeks of injections, mRNA  
291 levels of *Tnfsf11* and *Il6* were significantly higher in both genotypes after PTH  
292 treatment (Figure 4A and 4B); this increase was not significantly affected by the  
293 genotype (two-way ANOVA interaction p values = 0.365 and 0.314, respectively).  
294 This indicated that among cells in the flushed femora, which would include  
295 osteoblasts at different stages of differentiation as well as osteocytes, are some  
296 cells that retain normal responses of these genes to PTH.

297  
298 Wntless (Wnt)-signaling is important for osteoblast differentiation and bone  
299 formation, and PTH has been shown to stimulate Wnt signaling by suppressing  
300 Dickkopf1 (*Dkk1*) and sclerostin (*Sost*) expression in the osteoblast lineage (Keller  
301 and Kneissel 2005; Yao, et al. 2011). For this reason, we quantified mRNA levels  
302 of *Dkk1* and *Sost* in flushed femurs. As expected, *Dkk1* mRNA levels were  
303 significantly lower in PTH-treated *Dmp1Cre.gp130<sup>w/w</sup>* femurs compared with  
304 untreated mice. However, *Dkk1* was not lower in femurs from PTH-treated  
305 *Dmp1Cre.gp130<sup>f/f</sup>* mice compared to controls (Figure 4C). *Sost* mRNA levels were  
306 slightly, but not significantly, lowered in response to PTH in *Dmp1Cre.gp130<sup>w/w</sup>*  
307 femora. *Dmp1Cre.gp130<sup>f/f</sup>* femora showed a lower level of *Sost* mRNA compared  
308 to vehicle treated *Dmp1Cre.gp130<sup>w/w</sup>* controls; with PTH treatment these mice  
309 showed a significant increase in *Sost* mRNA levels (Figure 4D). These differences  
310 in effects of PTH treatment on gene expression were significant by two-way  
311 ANOVA for both *Dkk1* (interaction p=0.01) and *Sost* (interaction p=0.003). Thus,  
312 PTH treatment does not decrease Wnt antagonist expression in *Dmp1Cre.gp130<sup>f/f</sup>*

313 mice, implying that gp130 signalling in osteocytes is important for the PTH effect  
314 on Wnt signaling inhibitors.

315

316 *Pth1r* expression is reduced in *DMP1Cre.gp130<sup>ff</sup>* mice and *gp130* deficient  
317 osteoblasts

318 Since many effects of PTH were blocked in *Dmp1Cre.gp130<sup>ff</sup>* mice we quantified  
319 *Pth1r* mRNA levels in flushed femurs from untreated 12-week-old  
320 *Dmp1Cre.gp130<sup>ff</sup>* and *Dmp1Cre.gp130<sup>w/w</sup>* mice. Surprisingly, *Pth1r* mRNA  
321 expression was 47% lower in *Dmp1Cre.gp130<sup>ff</sup>* compared to *Dmp1Cre.gp130<sup>w/w</sup>*  
322 femurs (p=0.03) (Figure 5A).

323

324 These findings were supported by *in vitro* data, where C57/BL6 and *gp130<sup>ff</sup>*  
325 calvarial osteoblasts were infected with lentiviral cre-recombinase. In cre-  
326 infected *gp130<sup>ff</sup>* osteoblasts, *gp130* was significantly lowered by 52%, and *Pth1r*  
327 mRNA was 84% lower than in infected C57/BL6 cells (Figure 5 B,C). mRNA  
328 levels of *Runx2*, *Osx* and *Alpl* were not significantly altered by cre-infection of  
329 *gp130<sup>ff</sup>* osteoblasts (Figure 5C), consistent with previously published mRNA  
330 levels of these genes in the femora of *DMP1Cre.gp130<sup>f/f</sup>* mice (Johnson, et al.  
331 2014a). This suggests that cells of the osteoblast lineage require signals  
332 mediated by gp130 to maintain PTH1R expression, and that a lack of PTH1R in  
333 *DMP1Cre* expressing cells is responsible for the reduced response to anabolic  
334 PTH treatment.



## 335 Discussion

336 This work demonstrates that PTH-induced osteoblast differentiation is  
337 dependent on gp130 expression in mature osteoblast lineage cells. gp130 is  
338 needed to maintain *Pth1r* expression in osteoblasts, and is required for PTH to  
339 suppress the Wnt-antagonists *Dkk1* and *Sost*. In contrast, gp130 expression by  
340 osteocytes is not required for PTH to stimulate mRNA levels of the pro-  
341 osteoclastogenic factors RANKL (*Tnfsf11*) and *Il6* in bone.

342  
343 The stimulatory effect of PTH on trabecular osteoblast numbers and mineralizing  
344 surface was completely ablated in *DMP1Cre.gp130<sup>ff</sup>* mice. This may, at least  
345 partly, be explained by the lack of a reduction in both Wnt signaling inhibitors  
346 *Sost* and *Dkk1* in response to PTH. Wnt signaling stimulates osteoblast  
347 differentiation, and it has been postulated that this is one pathway through  
348 which PTH stimulates bone formation (Kulkarni, et al. 2005), a hypothesis  
349 supported by impaired PTH responses in mice overexpressing sclerostin or *Dkk1*  
350 (Guo, et al. 2010; Kramer, et al. 2010). PTH directly inhibits *Sost* via cAMP-PKA  
351 signaling (Keller and Kneissel 2005). IL-6 family cytokines also rapidly inhibit  
352 *Sost*, although the mechanism remains unknown (Walker et al. 2010). Whether  
353 the reduction in effect of PTH on Wnt signaling is entirely due to the reduced  
354 PTH1R expression or results from some dependence on gp130 cytokines on this  
355 same pathway in osteoblasts and osteocytes remains unclear.

356  
357 In contrast to the effect on Wnt-antagonists, both *Dmp1Cre.gp130<sup>w/w</sup>* and  
358 *Dmp1Cre.gp130<sup>ff</sup>* mice demonstrated increased femoral *Rankl* and *Il6* mRNA

359 levels in response to PTH. Despite these increases in both genotypes, osteoclast  
360 numbers were unchanged, as we have previously reported with this low dose of  
361 intermittent PTH treatment (Takyar et al. 2013; Tonna et al. 2014), likely  
362 because the inductions of RANKL and IL-6 are transient (Ma, et al. 2001; Walker  
363 et al. 2012). Il-6 and RANKL are expressed by a wide range of cells in the bone,  
364 including osteoblast lineage cells as well as osteocytes (Dai, et al. 2006; Lee and  
365 Lorenzo 1999; Nakashima, et al. 2011; Xiong et al. 2011), but also cells within the  
366 bone marrow, including T-cells (Horwood, et al. 1999; Matthews, et al. 2014)  
367 and, in the case of IL-6, macrophages (Balic and Mina 2011). Although PTH has  
368 recently been suggested to directly promote RANKL expression in osteocytes  
369 (Xiong et al. 2011), our findings suggest that the major cellular targets that  
370 produce these pro-osteoclastogenic factors in response to PTH are not  
371 osteocytes. Notably, although PTH was unable to increase osteoblast numbers or  
372 mineralizing surface in the *Dmp1Cre.gp130<sup>fl/fl</sup>* mice, on those surfaces where  
373 double calcein labels were incorporated into the bone matrix, the distance  
374 between them (MAR) was significantly greater in PTH treated mice, regardless of  
375 genotype. This suggests that those bone-forming osteoblasts that are on the bone  
376 surface in *Dmp1Cre.gp130<sup>fl/fl</sup>* mice retain sufficient PTHR expression to respond to  
377 PTH with increased matrix production. Since marrow was flushed from the  
378 femora, and *Pth1r* levels were dramatically reduced in undifferentiated cultured  
379 cre-expressing cells, we suggest that the key PTH-responsive cells producing  
380 RANKL and IL-6 in this model are less differentiated osteoblasts, not expressing  
381 DMP1Cre, on the bone surface.  
382

383 *Pth1r* mRNA was lower in cortical bone from mice lacking gp130 in osteocytes  
384 (*Dmp1Cre.gp130<sup>ff</sup>*) compared with littermate controls, an effect that was  
385 reproduced when gp130 was deleted in cultured primary calvarial osteoblasts.  
386 There are two ways to understand this: firstly, since osteoblast differentiation is  
387 impaired in the *Dmp1Cre.gp130<sup>ff</sup>* mice (Johnson et al. 2014a), and PTH1R  
388 expression in the osteoblast lineage is higher in more mature osteoblasts (Allan  
389 et al. 2008; Allan, et al. 2003; Balic, et al. 2010), there may be fewer mature  
390 PTH1R-expressing osteoblasts present within the bone of these mice. Another  
391 interpretation is that gp130 is needed to maintain the expression of PTH1R in  
392 the osteoblast lineage. This latter hypothesis is supported by our *in vitro* data,  
393 since we observed that a reduction of gp130 by about 50% in calvarial  
394 osteoblasts cultured *in vitro* reduced *Pth1r* mRNA by nearly 80%. This further  
395 suggests that as well as maintaining PTH1R levels in the osteocyte, gp130 may  
396 maintain PTH1R expression in throughout the osteoblast lineage.

397  
398 Although *Pth1r* levels were low in the femora of *Dmp1Cre.gp130<sup>ff</sup>* mice, their  
399 phenotype is strikingly different to mice with a conditional deletion of PTH1R in  
400 osteocytes (Ocy-PPRKO), generated using the same DMP1Cre (Saini, et al. 2013).  
401 Ocy-PPRKO mice showed a greater trabecular bone mass than controls with no  
402 significant alteration in osteoblast numbers, indicating that the underlying cause  
403 of bone fragility in the *Dmp1Cre.gp130<sup>ff</sup>* mice is not simply low PTH1R  
404 expression in the osteocyte. As observed in *Dmp1Cre.gp130<sup>ff</sup>* mice, Ocy-PPRKO  
405 mice failed to reduce *Sost* in response to PTH treatment. However, in direct  
406 contrast to *Dmp1Cre.gp130<sup>ff</sup>* mice, Ocy-PPRKO lacked a *Tnfsf11* response to PTH.

407 This suggests that the *Dkk1/Sost* and *Tnfsf11/Il6st* responses to PTH occur in  
408 different cell populations, and it is only the former that is affected by DMP1Cre-  
409 mediated gp130 deletion. Alternatively, the *Dkk1/Sost* induction may require a  
410 higher level of PTH1R expression than the *Tnfsf11/Il6st* response; the low level  
411 of PTH1R expression in the *Dmp1Cre.gp130<sup>ff</sup>* mice may be sufficient for the  
412 latter.

413

414 In addition to mediating the response of osteoblasts to exogenous PTH  
415 treatment, PTH1R also acts as a receptor for parathyroid hormone related  
416 protein (PTHrP). Although first identified as the mediator of humoral  
417 hypercalcemia of malignancy (Suva, et al. 1987), PTHrP is also produced by the  
418 osteoblast lineage (Kartsogiannis, et al. 1997; Sackmann 1995). This local PTHrP  
419 production is essential for normal osteoblast differentiation, as indicated by  
420 studies of an osteoblast-lineage PTHrP null mouse (Miao, et al. 2005). This  
421 suggests that basal defects in osteoblast differentiation in our model lacking  
422 gp130 in osteocytes may relate specifically to a lack of PTHrP signal. Notably,  
423 and in direct contrast to our model, the osteoblast-lineage knockout of PTHrP  
424 also exhibited a significant impairment in osteoclastogenesis (Miao et al. 2005), a  
425 finding that may relate to the difference in the gene driving expression of the  
426 Cre-recombinase. The PTHrP<sup>ff</sup> deletion was driven by the Col2.3Cre, which  
427 would delete expression in osteocytes, but also in less mature osteoblasts than  
428 the DMP1Cre that we have used. Again, this suggests that the PTH-induced  
429 expression of RANKL is likely to occur in less mature osteoblasts.

430

431 In conclusion, in addition to the recently described role of osteocytic gp130 in  
432 maintaining bone formation and strength (Johnson et al. 2014a), the current  
433 study has revealed a new role for gp130 in the osteoblast lineage in bone: it is  
434 needed to maintain PTH1R expression and to increase osteoblast numbers in  
435 response to anabolic PTH treatment.

For Review Only

## 436 **Funding**

437 Funding sources: This work was supported by a National Health and Medical  
438 Research Council (Australia) Project Grant 1002728. N.A.S. is supported by a  
439 National Health and Medical Research Council (Australia) Senior Research  
440 Fellowship. TS is supported by a Senior Research Fellowship from the Norwegian  
441 Cancer Society (project number 538153). The Victorian State Government  
442 Operational Infrastructure Support Scheme provides support to St. Vincent's  
443 Institute of Medical Research.

## 444 **Author contributions**

445 Study design: NAS, TS. Study conduct and data collection: TS, RWJ, NEM, IJP,  
446 PWMH. Data analysis: TS, RWJ, NEM, IJP, PWMH, NAS. Data interpretation: TS,  
447 RWJ, NEM, IJP, PWMH, TJM, NAS. Drafting manuscript: TS and NAS. Revising  
448 manuscript content: TS, NAS, RWJ, TJM. All authors approved the final version of  
449 manuscript. NAS takes responsibility for the integrity of the data analysis.

## 450 **Acknowledgements**

451 We thank Joshua Johnson for technical expertise in the processing of bone  
452 samples for histomorphometric analysis, Dr. Stephen Tonna for advice on  
453 Lentiviral Cre infection, and Dr. Nicole Walsh for design of the *Dkk1* primers.

454 **References**

- 455 Allan EH, Hausler KD, Wei T, Gooi JH, Quinn JM, Crimeen-Irwin B, Pompolo S,  
456 Sims NA, Gillespie MT, Onyia JE, et al. 2008 EphrinB2 regulation by PTH and  
457 PTHrP revealed by molecular profiling in differentiating osteoblasts. *J Bone*  
458 *Miner Res* **23** 1170-1181.
- 459 Allan EH, Ho PW, Umezawa A, Hata J, Makishima F, Gillespie MT & Martin TJ  
460 2003 Differentiation potential of a mouse bone marrow stromal cell line. *J Cell*  
461 *Biochem* **90** 158-169.
- 462 Balic A, Aguila HL & Mina M 2010 Identification of cells at early and late stages of  
463 polarization during odontoblast differentiation using pOBCol3.6GFP and  
464 pOBCol2.3GFP transgenic mice. *Bone* **47** 948-958.
- 465 Balic A & Mina M 2011 Identification of secretory odontoblasts using DMP1-GFP  
466 transgenic mice. *Bone* **48** 927-937.
- 467 Bellido T, Ali AA, Gubrij I, Plotkin LI, Fu Q, O'Brien CA, Manolagas SC & Jilka RL  
468 2005 Chronic elevation of parathyroid hormone in mice reduces expression of  
469 sclerostin by osteocytes: a novel mechanism for hormonal control of  
470 osteoblastogenesis. *Endocrinology* **146** 4577-4583.
- 471 Betz UA, Bloch W, van den Broek M, Yoshida K, Taga T, Kishimoto T, Addicks K,  
472 Rajewsky K & Muller W 1998 Postnatally induced inactivation of gp130 in mice  
473 results in neurological, cardiac, hematopoietic, immunological, hepatic, and  
474 pulmonary defects. *J Exp Med* **188** 1955-1965.
- 475 Cornish J, Callon K, King A, Edgar S & Reid IR 1993 The effect of leukemia  
476 inhibitory factor on bone in vivo. *Endocrinology* **132** 1359-1366.
- 477 Dai JC, He P, Chen X & Greenfield EM 2006 TNFalpha and PTH utilize distinct  
478 mechanisms to induce IL-6 and RANKL expression with markedly different  
479 kinetics. *Bone* **38** 509-520.

- 480 Dobnig H & Turner RT 1995 Evidence that intermittent treatment with  
481 parathyroid hormone increases bone formation in adult rats by activation of  
482 bone lining cells. *Endocrinology* **136** 3632-3638.
- 483 Greenfield EM, Horowitz MC & Lavish SA 1996 Stimulation by parathyroid  
484 hormone of interleukin-6 and leukemia inhibitory factor expression in  
485 osteoblasts is an immediate-early gene response induced by cAMP signal  
486 transduction. *J Biol Chem* **271** 10984-10989.
- 487 Greenfield EM, Shaw SM, Gornik SA & Banks MA 1995 Adenyl cyclase and  
488 interleukin 6 are downstream effectors of parathyroid hormone resulting in  
489 stimulation of bone resorption. *J Clin Invest* **96** 1238-1244.
- 490 Guo J, Liu M, Yang D, Bouxsein ML, Saito H, Galvin RJ, Kuhstoss SA, Thomas CC,  
491 Schipani E, Baron R, et al. 2010 Suppression of Wnt signaling by Dkk1 attenuates  
492 PTH-mediated stromal cell response and new bone formation. *Cell Metab* **11**  
493 161-171.
- 494 Hodsman AB, Bauer DC, Dempster DW, Dian L, Hanley DA, Harris ST, Kendler DL,  
495 McClung MR, Miller PD, Olszynski WP, et al. 2005 Parathyroid hormone and  
496 teriparatide for the treatment of osteoporosis: a review of the evidence and  
497 suggested guidelines for its use. *Endocr Rev* **26** 688-703.
- 498 Horwood NJ, Kartsogiannis V, Quinn JM, Romas E, Martin TJ & Gillespie MT 1999  
499 Activated T lymphocytes support osteoclast formation in vitro. *Biochem Biophys*  
500 *Res Commun* **265** 144-150.
- 501 Jilka RL, Weinstein RS, Bellido T, Roberson P, Parfitt AM & Manolagas SC 1999  
502 Increased bone formation by prevention of osteoblast apoptosis with  
503 parathyroid hormone. *J Clin Invest* **104** 439-446.
- 504 Johnson RW, Brennan HJ, Vrahnas C, Poulton IJ, McGregor NE, Standal T, Walker  
505 EC, Koh TT, Nguyen H, Walsh NC, et al. 2014a The Primary Function of gp130  
506 Signaling in Osteoblasts Is To Maintain Bone Formation and Strength, Rather  
507 Than Promote Osteoclast Formation. *J Bone Miner Res* **29** 1492-1505.



- 508 Johnson RW, White JD, Walker EC, Martin TJ & Sims NA 2014b Myokines  
509 (muscle-derived cytokines and chemokines) including ciliary neurotrophic factor  
510 (CNTF) inhibit osteoblast differentiation. *Bone* **64C** 47-56.
- 511 Kartsogiannis V, Moseley J, McKelvie B, Chou ST, Hards DK, Ng KW, Martin TJ &  
512 Zhou H 1997 Temporal expression of PTHrP during endochondral bone  
513 formation in mouse and intramembranous bone formation in an in vivo rabbit  
514 model. *Bone* **21** 385-392.
- 515 Keller H & Kneissel M 2005 SOST is a target gene for PTH in bone. *Bone* **37** 148-  
516 158.
- 517 Khosla S, Westendorf JJ & Oursler MJ 2008 Building bone to reverse osteoporosis  
518 and repair fractures. *J Clin Invest* **118** 421-428.
- 519 Kim SW, Pajevic PD, Selig M, Barry KJ, Yang JY, Shin CS, Baek WY, Kim JE &  
520 Kronenberg HM 2012 Intermittent parathyroid hormone administration  
521 converts quiescent lining cells to active osteoblasts. *J Bone Miner Res* **27** 2075-  
522 2084.
- 523 Kramer I, Loots GG, Studer A, Keller H & Kneissel M 2010 Parathyroid hormone  
524 (PTH)-induced bone gain is blunted in SOST overexpressing and deficient mice. *J*  
525 *Bone Miner Res* **25** 178-189.
- 526 Kulkarni NH, Halladay DL, Miles RR, Gilbert LM, Frolik CA, Galvin RJ, Martin TJ,  
527 Gillespie MT & Onyia JE 2005 Effects of parathyroid hormone on Wnt signaling  
528 pathway in bone. *J Cell Biochem* **95** 1178-1190.
- 529 Lee SK & Lorenzo JA 1999 Parathyroid hormone stimulates TRANCE and inhibits  
530 osteoprotegerin messenger ribonucleic acid expression in murine bone marrow  
531 cultures: correlation with osteoclast-like cell formation. *Endocrinology* **140**  
532 3552-3561.
- 533 Lindsay R, Zhou H, Cosman F, Nieves J, Dempster DW & Hodsman AB 2007  
534 Effects of a one-month treatment with PTH(1-34) on bone formation on

- 535 cancellous, endocortical, and periosteal surfaces of the human ilium. *J Bone Miner*  
536 *Res* **22** 495-502.
- 537 Lu Y, Xie Y, Zhang S, Dusevich V, Bonewald LF & Feng JQ 2007 DMP1-targeted  
538 Cre expression in odontoblasts and osteocytes. *J Dent Res* **86** 320-325.
- 539 Ma YL, Cain RL, Halladay DL, Yang X, Zeng Q, Miles RR, Chandrasekhar S, Martin  
540 TJ & Onyia JE 2001 Catabolic effects of continuous human PTH (1--38) in vivo is  
541 associated with sustained stimulation of RANKL and inhibition of  
542 osteoprotegerin and gene-associated bone formation. *Endocrinology* **142** 4047-  
543 4054.
- 544 Matthews BG, Grcevic D, Wang L, Hagiwara Y, Roguljic H, Joshi P, Shin DG, Adams  
545 DJ & Kalajzic I 2014 Analysis of alphaSMA-labeled progenitor cell commitment  
546 identifies notch signaling as an important pathway in fracture healing. *J Bone*  
547 *Miner Res* **29** 1283-1294.
- 548 McGregor NE, Poulton IJ, Walker EC, Pompolo S, Quinn JM, Martin TJ & Sims NA  
549 2010 Ciliary neurotrophic factor inhibits bone formation and plays a sex-specific  
550 role in bone growth and remodeling. *Calcif Tissue Int* **86** 261-270.
- 551 Miao D, He B, Jiang Y, Kobayashi T, Soroceanu MA, Zhao J, Su H, Tong X, Amizuka  
552 N, Gupta A, et al. 2005 Osteoblast-derived PTHrP is a potent endogenous bone  
553 anabolic agent that modifies the therapeutic efficacy of administered PTH 1-34. *J*  
554 *Clin Invest* **115** 2402-2411.
- 555 Nakashima T, Hayashi M, Fukunaga T, Kurata K, Oh-Hora M, Feng JQ, Bonewald  
556 LF, Kodama T, Wutz A, Wagner EF, et al. 2011 Evidence for osteocyte regulation  
557 of bone homeostasis through RANKL expression. *Nat Med* **17** 1231-1234.
- 558 Neer RM, Arnaud CD, Zanchetta JR, Prince R, Gaich GA, Reginster JY, Hodsman  
559 AB, Eriksen EF, Ish-Shalom S, Genant HK, et al. 2001 Effect of parathyroid  
560 hormone (1-34) on fractures and bone mineral density in postmenopausal  
561 women with osteoporosis. *N Engl J Med* **344** 1434-1441.

- 562 O'Brien CA, Gubrij I, Lin SC, Saylor RL & Manolagas SC 1999 STAT3 activation in  
563 stromal/osteoblastic cells is required for induction of the receptor activator of  
564 NF-kappaB ligand and stimulation of osteoclastogenesis by gp130-utilizing  
565 cytokines or interleukin-1 but not 1,25-dihydroxyvitamin D3 or parathyroid  
566 hormone. *J Biol Chem* **274** 19301-19308.
- 567 Palmqvist P, Persson E, Conaway HH & Lerner UH 2002 IL-6, leukemia inhibitory  
568 factor, and oncostatin M stimulate bone resorption and regulate the expression  
569 of receptor activator of NF-kappa B ligand, osteoprotegerin, and receptor  
570 activator of NF-kappa B in mouse calvariae. *J Immunol* **169** 3353-3362.
- 571 Parfitt AM, Drezner MK, Glorieux FH, Kanis JA, Malluche H, Meunier PJ, Ott SM &  
572 Recker RR 1987 Bone histomorphometry: standardization of nomenclature,  
573 symbols, and units. Report of the ASBMR Histomorphometry Nomenclature  
574 Committee. *J Bone Miner Res* **2** 595-610.
- 575 Reeve J, Meunier PJ, Parsons JA, Bernat M, Bijvoet OL, Courpron P, Edouard C,  
576 Klenerman L, Neer RM, Renier JC, et al. 1980 Anabolic effect of human  
577 parathyroid hormone fragment on trabecular bone in involutional osteoporosis:  
578 a multicentre trial. *Br Med J* **280** 1340-1344.
- 579 Richards CD, Langdon C, Deschamps P, Pennica D & Shaughnessy SG 2000  
580 Stimulation of osteoclast differentiation in vitro by mouse oncostatin M,  
581 leukaemia inhibitory factor, cardiotrophin-1 and interleukin 6: synergy with  
582 dexamethasone. *Cytokine* **12** 613-621.
- 583 Romas E, Udagawa N, Zhou H, Tamura T, Saito M, Taga T, Hilton DJ, Suda T, Ng  
584 KW & Martin TJ 1996 The role of gp130-mediated signals in osteoclast  
585 development: regulation of interleukin 11 production by osteoblasts and  
586 distribution of its receptor in bone marrow cultures. *J Exp Med* **183** 2581-2591.
- 587 Sackmann E 1995 Biological Membranes Architecture and Function. In *Handbook*  
588 *of Biological Physics, Vol. 1*. Eds R Lipowsky & E Sackmann: Elsevier.

- 589 Saini V, Marengi DA, Barry KJ, Fulzele KS, Heiden E, Liu X, Dedic C, Maeda A,  
590 Lotinun S, Baron R, et al. 2013 Parathyroid hormone (PTH)/PTH-related peptide  
591 type 1 receptor (PPR) signaling in osteocytes regulates anabolic and catabolic  
592 skeletal responses to PTH. *J Biol Chem* **288** 20122-20134.
- 593 Sims NA, Brennan K, Spaliviero J, Handelsman DJ & Seibel MJ 2006 Perinatal  
594 testosterone surge is required for normal adult bone size but not for normal  
595 bone remodeling. *Am J Physiol Endocrinol Metab* **290** E456-462.
- 596 Sims NA & Walsh NC 2010 GP130 cytokines and bone remodelling in health and  
597 disease. *BMB Rep* **43** 513-523.
- 598 Suva LJ, Winslow GA, Wettenhall RE, Hammonds RG, Moseley JM, Diefenbach-  
599 Jagger H, Rodda CP, Kemp BE, Rodriguez H, Chen EY, et al. 1987 A parathyroid  
600 hormone-related protein implicated in malignant hypercalcemia: cloning and  
601 expression. *Science* **237** 893-896.
- 602 Takyar FM, Tonna S, Ho PW, Crimeen-Irwin B, Baker EK, Martin TJ & Sims NA  
603 2013 EphrinB2/EphB4 inhibition in the osteoblast lineage modifies the anabolic  
604 response to parathyroid hormone. *J Bone Miner Res* **28** 912-925.
- 605 Tamura T, Udagawa N, Takahashi N, Miyaura C, Tanaka S, Yamada Y, Koishihara  
606 Y, Ohsugi Y, Kumaki K, Taga T, et al. 1993 Soluble interleukin-6 receptor triggers  
607 osteoclast formation by interleukin 6. *Proc Natl Acad Sci U S A* **90** 11924-11928.
- 608 Tonna S, Takyar FM, Vrahnas C, Crimeen-Irwin B, Ho PW, Poulton IJ, Brennan HJ,  
609 McGregor NE, Allan EH, Nguyen H, et al. 2014 EphrinB2 signaling in osteoblasts  
610 promotes bone mineralization by preventing apoptosis. *FASEB J*.
- 611 Torreggiani E, Matthews BG, Pejda S, Matic I, Horowitz MC, Grcevic D & Kalajzic I  
612 2013 Preosteocytes/osteocytes have the potential to dedifferentiate becoming a  
613 source of osteoblasts. *PLoS One* **8** e75204.
- 614 Udagawa N, Takahashi N, Jimi E, Matsuzaki K, Tsurukai T, Itoh K, Nakagawa N,  
615 Yasuda H, Goto M, Tsuda E, et al. 1999 Osteoblasts/stromal cells stimulate

616 osteoclast activation through expression of osteoclast differentiation  
617 factor/RANKL but not macrophage colony-stimulating factor: receptor activator  
618 of NF-kappa B ligand. *Bone* **25** 517-523.

619 Walker EC, McGregor NE, Poulton IJ, Pompolo S, Allan EH, Quinn JM, Gillespie MT,  
620 Martin TJ & Sims NA 2008 Cardiotrophin-1 is an osteoclast-derived stimulus of  
621 bone formation required for normal bone remodeling. *J Bone Miner Res* **23** 2025-  
622 2032.

623 Walker EC, McGregor NE, Poulton IJ, Solano M, Pompolo S, Fernandes TJ,  
624 Constable MJ, Nicholson GC, Zhang JG, Nicola NA, et al. 2010 Oncostatin M  
625 promotes bone formation independently of resorption when signaling through  
626 leukemia inhibitory factor receptor in mice. *J Clin Invest* **120** 582-592.

627 Walker EC, Poulton IJ, McGregor NE, Ho PW, Allan EH, Quach JM, Martin TJ &  
628 Sims NA 2012 Sustained RANKL response to parathyroid hormone in oncostatin  
629 M receptor-deficient osteoblasts converts anabolic treatment to a catabolic effect  
630 in vivo. *J Bone Miner Res* **27** 902-912.

631 Xiong J, Onal M, Jilka RL, Weinstein RS, Manolagas SC & O'Brien CA 2011 Matrix-  
632 embedded cells control osteoclast formation. *Nat Med* **17** 1235-1241.

633 Yao GQ, Wu JJ, Troiano N & Insogna K 2011 Targeted overexpression of Dkk1 in  
634 osteoblasts reduces bone mass but does not impair the anabolic response to  
635 intermittent PTH treatment in mice. *J Bone Miner Metab* **29** 141-148.

636

## 637 **Figure legends**

638 **Figure 1. Osteocytic gp130 is required for PTH to increase osteoblast**  
639 **numbers and bone formation in trabecular bone.** Male mice were treated  
640 with hPTH (1-34) at 30µg/kg/day for 5 weeks. Shown are (A) numbers of  
641 osteoblasts / bone perimeter (N.Ob/B.Pm), (B) osteoblast surface / bone surface

642 (Ob.S/BS) and (C) osteoid surface / bone surface (OS/BS), (D) osteoid thickness  
643 (OTh), (E) Double calcein labeled surface (dLS/BS) and (F) mineral apposition  
644 rate (MAR) from trabecular bone in the proximal tibial secondary spongiosa in  
645 *Dmp1Cre.gp130<sup>w/w</sup>* (gp130 w/w) and *Dmp1Cre.gp130<sup>f/f</sup>* (gp130 f/f) mice. (G)  
646 Serum levels of procollagen type 1 amino-terminal propeptide (P1NP) and (H)  
647 endogenous murine PTH measured at the end of the treatment protocol are also  
648 shown. Bars are mean + SEM, n=8-10 per group. \* p≤ 0.05, \*\* p≤ 0.01, \*\*\* p≤  
649 0.001, PTH-treated compared to genotype-matched vehicle treated mice.

650

651 **Figure 2. No effect of intermittent PTH on bone resorption.** Male mice were  
652 treated with hPTH (1-34) at 30µg/kg/day for 5 weeks. Shown are (A) numbers  
653 of osteoclasts per unit bone perimeter (NOc/BPm), (B) osteoclast surface per  
654 unit bone surface (OcS/BS) measured in the proximal tibial secondary spongiosa,  
655 and (C) serum levels of cross-linked C-terminal telopeptide of type I collagen  
656 (CTX1) in PTH and vehicle treated *Dmp1Cre.gp130<sup>w/w</sup>* (gp130 w/w) and  
657 *Dmp1Cre.gp130<sup>f/f</sup>* (gp130 f/f) mice. Bars are mean + SEM, n=8-10 per group.

658

659 **Figure 3. PTH effects on cortical bone are impaired in *Dmp1Cre.gp130<sup>f/f</sup>***  
660 **mice.**

661 Male mice were treated with hPTH (1-34) at 30µg/kg/day for 5 weeks. Shown  
662 are (A) tibial periosteal double-labeled surface (Ps.dLS/BS), periosteal mineral  
663 apposition rate (Ps.MAR) in the tibial diaphysis and (C) periosteal perimeter  
664 (Ps.Pm) of the femoral diaphysis in PTH and vehicle treated *Dmp1Cre.gp130<sup>w/w</sup>*  
665 (gp130 w/w) and *Dmp1Cre.gp130<sup>f/f</sup>* (gp130 f/f) mice. Bars are mean + SEM, n=8-

666 10 per group. \*\*  $p \leq 0.01$ , ns,  $p > 0.05$  (not statistically significant) in PTH-treated  
667 compared to genotype-matched vehicle-treated mice. +,  $p < 0.05$ , vehicle-treated  
668 *Dmp1Cre.gp130<sup>ff</sup>* compared to vehicle-treated *Dmp1Cre.gp130<sup>w/w</sup>*.

669

670 **Figure 4. PTH effects on Wnt-inhibitor, but not osteoclastogenic, mRNA**

671 **levels are impaired in *DMP1Cre.gp130<sup>ff</sup>* mice.** RNA was isolated from femurs  
672 flushed of bone marrow and expression of PTH target genes was examined by  
673 relative quantitative PCR. *Tnfs11* mRNA (A), *Il-6* mRNA (B), *Dkk1* mRNA (C) and  
674 *Sost* mRNA (D) in *Dmp1Cre.gp130<sup>w/w</sup>* and *Dmp1Cre.gp130<sup>ff</sup>* mice treated for five  
675 weeks with PTH, collected one hour after the final injection. All values are shown  
676 relative to housekeeping (HKG) - the geometric mean of hypoxanthine  
677 phosphoribosyltransferase 1 (*Hprt1*) and hydroxymethylbilane synthase  
678 (*Hmbs*). Bars are mean + SEM,  $n=5-8$  bones per group, with mRNA prepared  
679 and analysed separately. \*\*  $p \leq 0.01$ , \*\*\*  $p \leq 0.001$ , PTH-treated compared to  
680 genotype-matched vehicle treated mice; +,  $p < 0.05$ , vehicle-treated  
681 *Dmp1Cre.gp130<sup>ff</sup>* compared to vehicle-treated *Dmp1Cre.gp130<sup>w/w</sup>*.

682

683 **Figure 5. PTH1R expression is reduced in *DMP1Cre.gp130<sup>ff</sup>* mice and gp130**

684 **deficient cultured osteoblasts.** (A) *Pth1r* mRNA quantified by qPCR in femurs  
685 flushed of bone marrow obtained from untreated 12-week old  
686 *Dmp1Cre.gp130<sup>w/w</sup>* and *Dmp1Cre.gp130<sup>ff</sup>* mice, normalized to *Hmbs*;  $n=8$  samples  
687 per group. (B) *gp130* (*Il6st*) and *Pth1r* mRNA levels in primary calvarial  
688 osteoblasts obtained from *gp130<sup>ff</sup>* or C57/BL6 wild type neonates infected with  
689 lentiviral Cre-recombinase; levels are shown normalised to beta-2-microglobulin

690 (B2m) (n=3 biological replicates). \*  $p \leq 0.05$ ; \*\*  $p \leq 0.01$ , vs gp130 w/w or  
691 C57/BL6.

For Review Only



692 **Table 1.** Effects of PTH on trabecular and cortical bone in femora from  
 693 *Dmp1Cre.gp130<sup>w/w</sup>* and *Dmp1Cre.gp130<sup>w/w</sup>* mice.

694

	<i>Dmp1Cre.gp130<sup>w/w</sup></i>		<i>Dmp1Cre.gp130<sup>f/f</sup></i>	
	Vehicle (n=9)	PTH (n=10)	Vehicle (n=9)	PTH (n=9)
BV/TV (%)	24.86 ± 0.42	21.54 ± 1.32	17.70 ± 1.55 <sup>+++</sup>	20.61 ± 0.96
Tb.Th (µm)	57.61 ± 1.80	56.49 ± 2.22	57.92 ± 3.01	57.42 ± 3.83
Tb.N (/mm)	4.35 ± 0.15	3.80 ± 0.16	3.03 ± 0.15 <sup>+++</sup>	3.64 ± 0.18
Tb.Sp (µm)	122.71 ± 2.96	144.39 ± 14.04	171.05 ± 15.74 <sup>+++</sup>	158.98 ± 10.37
Ct.Ar (mm <sup>2</sup> )	0.60 ± 0.02	0.65 ± 0.02	0.63 ± 0.02	0.67 ± 0.03

695 Fixed nondemineralized femora from vehicle or PTH-treated mice were analyzed  
 696 by µCT. Effect of PTH treatment: \*, p<0.05 vs *Dmp1Cre.gp130<sup>w/w</sup>*. Effect of  
 697 *gp130<sup>f/f</sup>* transgene: \*\*\* p< 0.001; \*, p<0.05 vs *Dmp1Cre.gp130<sup>w/w</sup>* (2-way ANOVA  
 698 with Šidak multiple comparisons test). BV/TV: bone volume per total volume of  
 699 the region of interest, Tb. Th: trabecular thickness, Tb. N: trabecular number,  
 700 Tb.Sp: trabecular separation; Ct.Ar: cortical area.

701

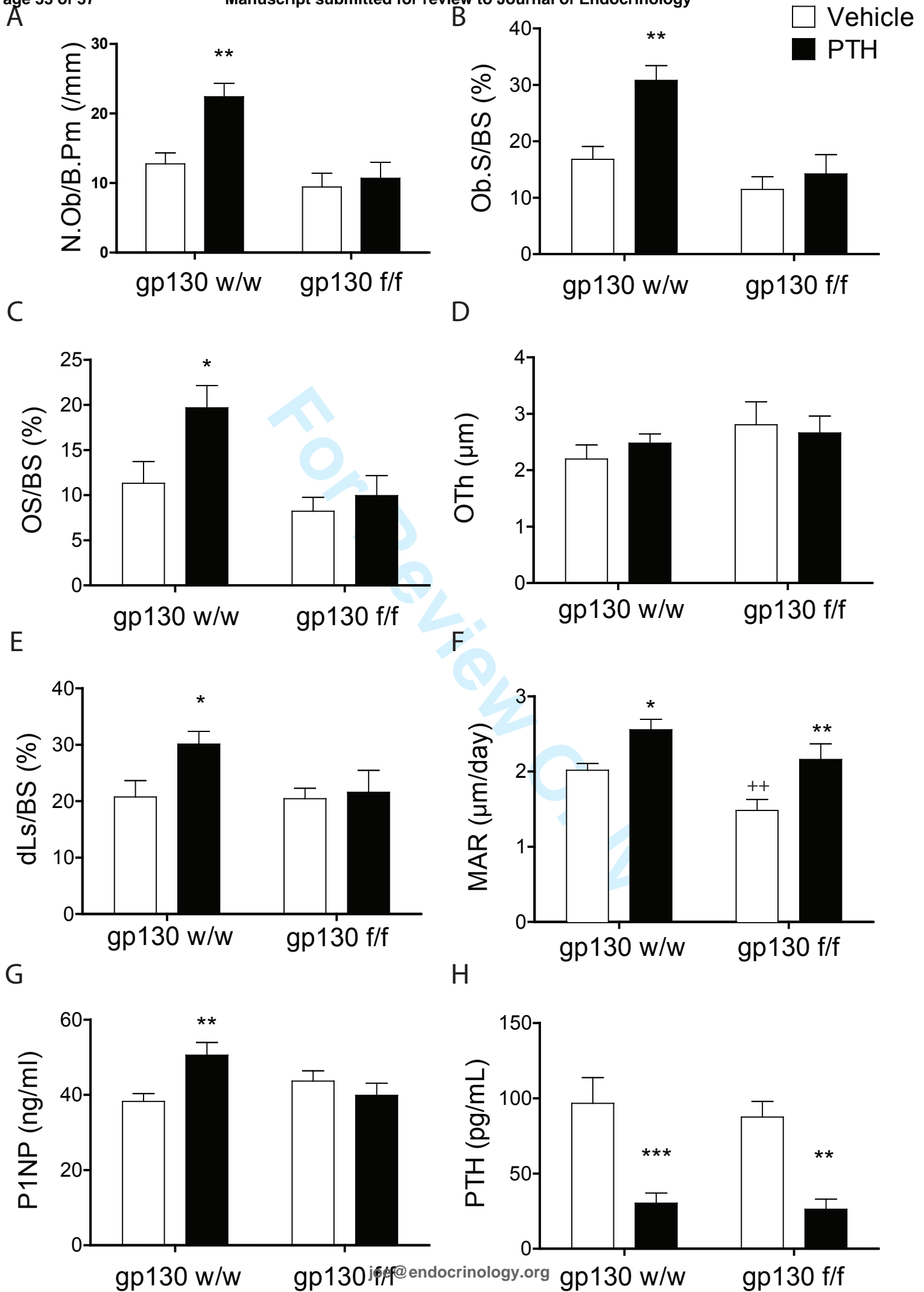
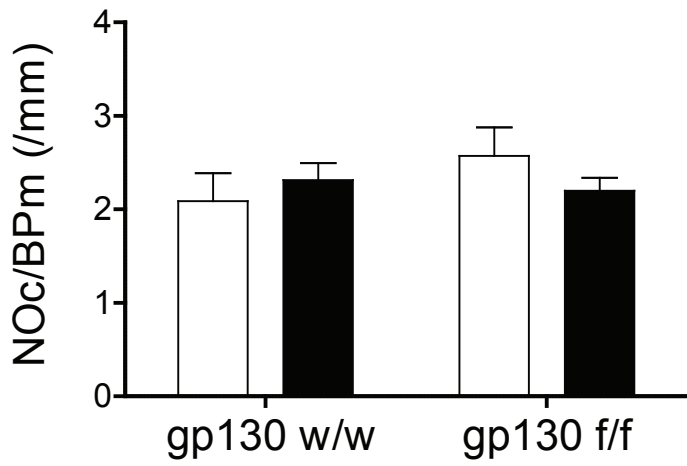
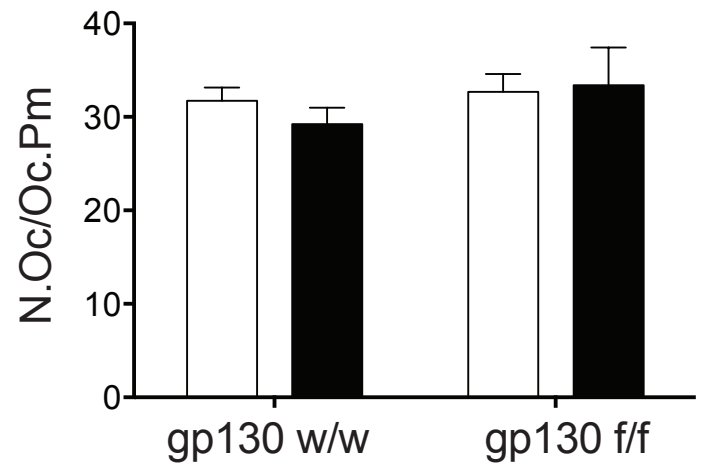


Figure 1

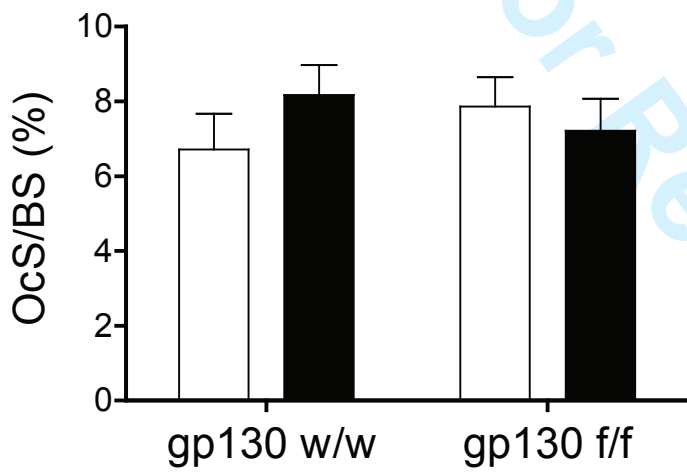
A



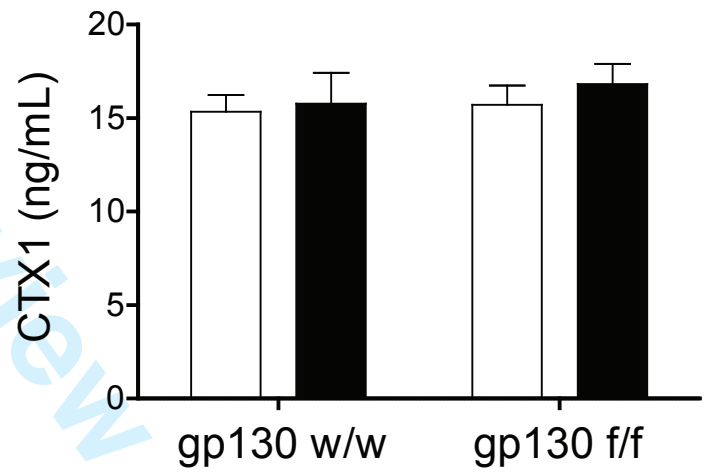
B



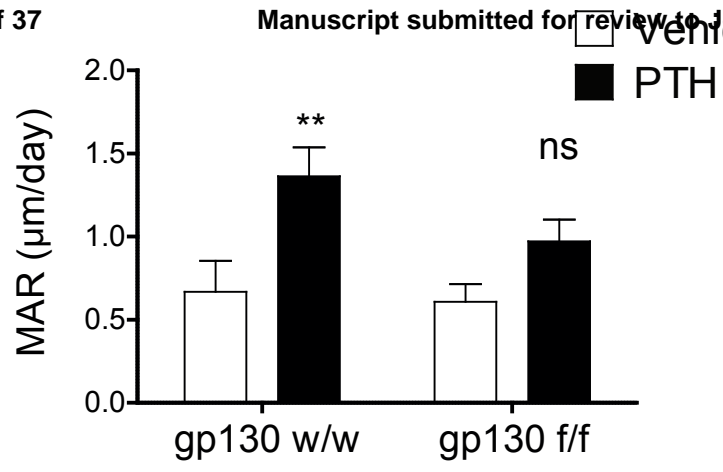
C



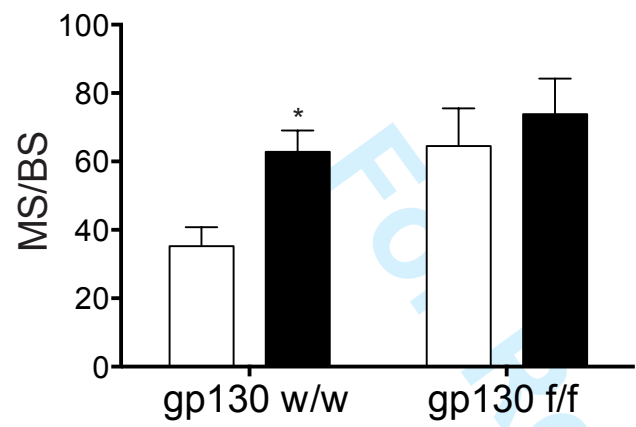
D



A



B



C

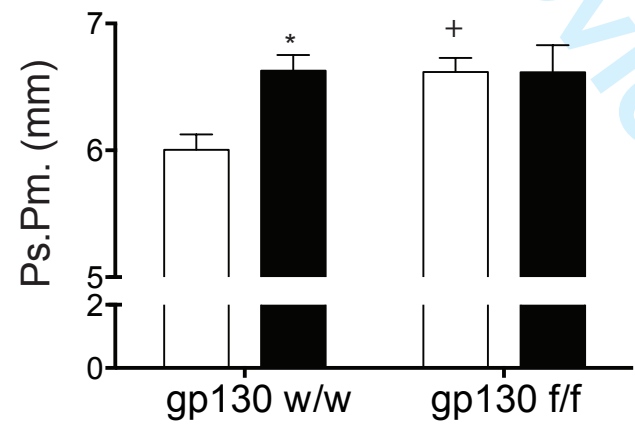
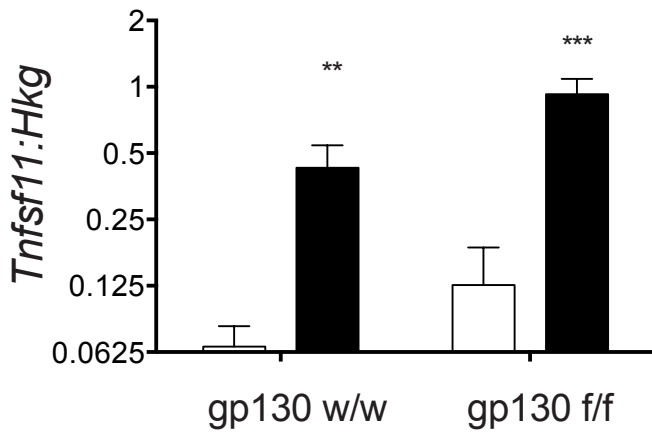
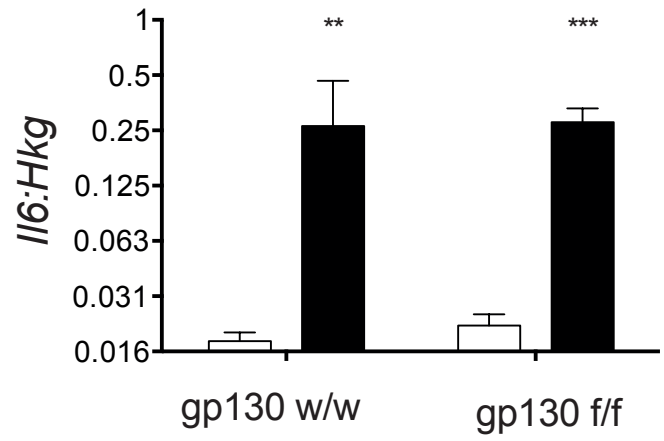


Figure 3

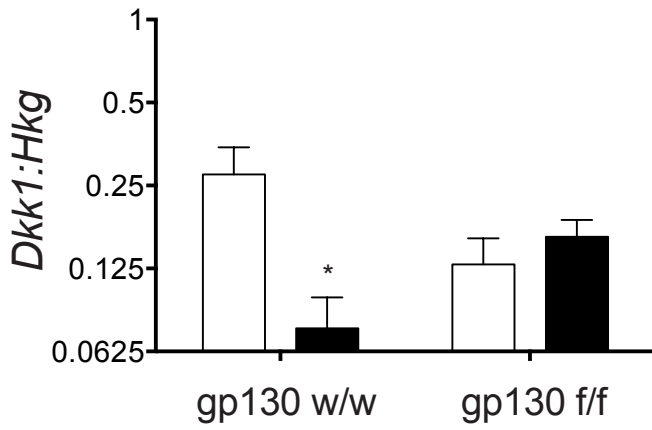
A



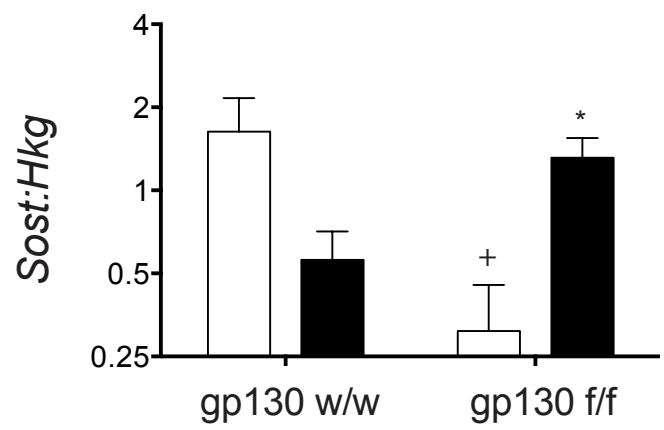
B



C

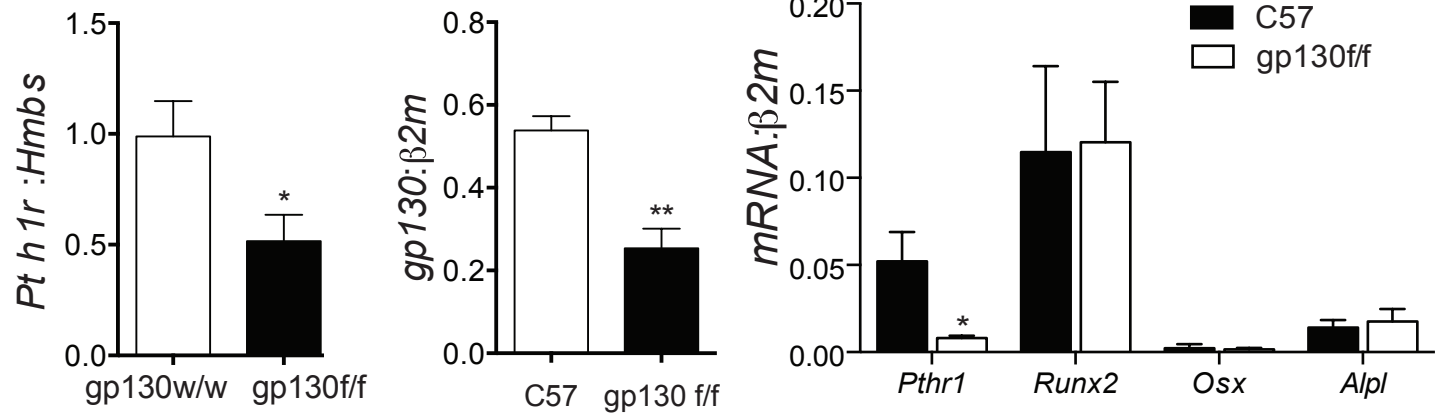


D



view Only

Figure 4



For Review Only